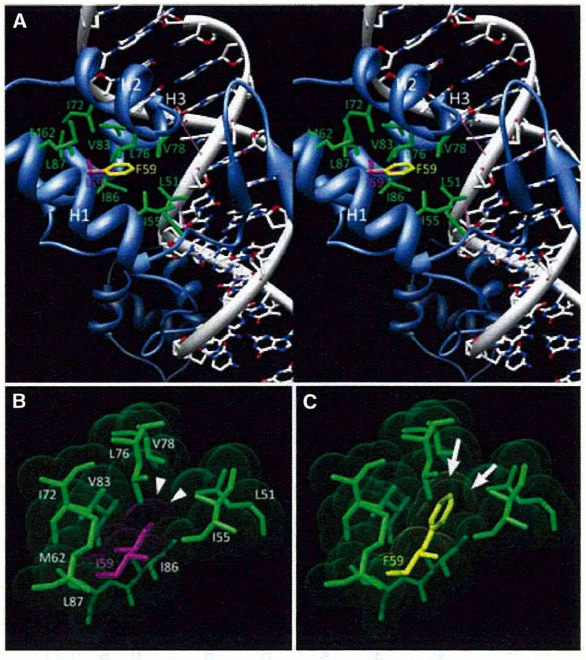

Figure 3. The predicted structure of the PAX3 paired domain-DNA complex. (A) The stereo view indicates that the mutated residue was surrounded by hydrophobic residues (green) protruding from H1, H2, and H3 of the paired domain (blue), which binds to DNA (white, sugar; blue, nitrogen; red, oxygen). The pink lines indicate hydrogen bonds. Magenta and yellow residues indicate I59 and F59, respectively. (B, C) The colored spheres indicate the van der Waals surface boundaries, the radius of the hydrophobic residues is shown in green, I59 is shown in magenta and is also indicated by arrowheads, and F59 is shown in yellow and is also indicated by arrows.

and her father had never been diagnosed with WS1. Pure tone audiometry of the proband showed severe hearing loss in the right ear and normal hearing in the left ear. The results of ABR and distortion product otoacoustic emissions in the proband were compatible with those obtained for pure tone audiometry.

Because direct sequencing of *PAX3* in the proband and her grandmother revealed no mutations, we conducted MLPA analysis to search for a large deletion of *PAX3*, and found that the copy number of all tested exons (exons 1–9) of *PAX3* was half that of the number of other chromosomal regions in both subjects (Figure 5A). In control subjects, all tested exons of *PAX3* showed the same copy number as the other chromosomal regions (Figure 5B). To determine the size of the deleted region, quantitative PCR was performed at 12 sequence-tagged sites on chromosome 2q36, which includes *PAX3*. In the proband, copy numbers at nine sites in the middle of the tested region (white arrows) were half that of those examined in normal controls, but the copy numbers at three of the sites near the 5' and 3' ends of the tested region (black arrows) were identical to those examined in normal controls (Figure 6). This result demonstrated that the chromosomal region spanning 1759–2554 kb at 2q36, which includes the whole *PAX3* gene, was deleted in one of the alleles of the proband. The same results were detected in the grandmother. A search for the deleted region revealed that this region contained between 12 and 18 genes, including *PAX3*.

Discussion

The heterozygous missense mutation, p.I59F, was identified in family 1. The pathogenicity of a novel or rare missense mutation in the causative gene is not necessarily verified even when the mutation is absent from a large number of normal controls, when the residue is evolutionary conserved among different species, or if the mutation is associated with the phenotype within a family, because an identified

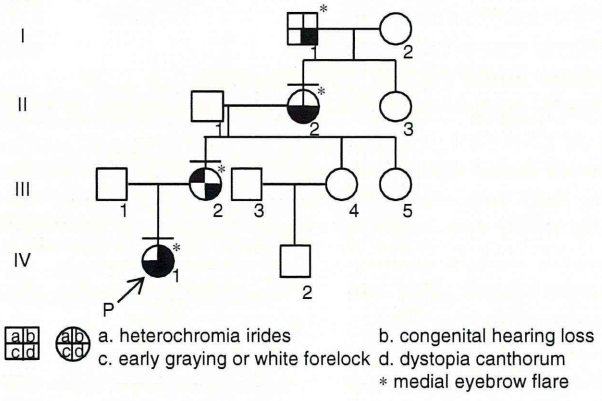

Figure 4. Pedigree of family 2. The proband is indicated by an arrow. The individuals we examined personally are indicated by a bar over the symbol. Phenotypes observed in this family are indicated symbolically, as detailed below the pedigree.

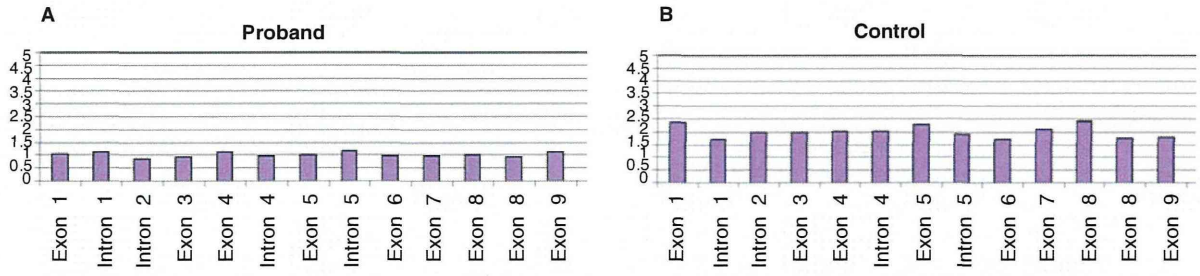

Figure 5. Results of MLPA analysis of *PAX3* in family 2. (A, B) Relative ratios of DNA quantity in each exon compared with that in the control region are shown for the proband (A) and control (B).

missense mutation may be a rare normal variant. Thus, the pathogenicity of such mutations needs to be verified by detection of the same mutation in multiple families with the same phenotype or by functional analysis. The functional consequences of a few *PAX3* mutations have been tested and reduced DNA-binding properties have been reported [13–15]. The p.I59F mutation was reported in a Japanese family [8], but functional analysis has not been conducted. We analyzed the predicted 3D structures of the paired domain of the PAX3-DNA complex and showed that this mutation was likely to distort the structure of the DNA-binding site of PAX3 and lead to functional impairment. This result substantially supports the hypothesis that the p.I59F mutation is pathogenic, although it is based on a theoretical prediction rather than functional experiments.

In family 2, the distinct phenotypes of the proband, the proband's mother, and the proband's grandmother were congenital unilateral hearing loss, heterochromia iridis, and early graying, respectively. Because of these differences, they were not aware of the hereditary nature of the symptoms. Identification of the *PAX3* mutation in the proband and the proband's grandmother led to an accurate diagnosis of WS1 and facilitated understanding of the symptoms. In this family, direct sequencing of *PAX3* did not detect any mutations, but MLPA analysis detected a large heterozygous deletion. Furthermore, quantitative PCR analysis revealed that the deleted region spanned 1759–2554 kb and included 12–18 genes. Large deletions of *PAX3* in patients with WS1 have been reported in several families [6,16–18]. To our knowledge, however, this is the largest deletion identified in patients with WS1 and has, therefore, expanded the spectrum of *PAX3* mutations. There is no reported correlation between the nature of the mutation (deleted vs truncated or missense) or

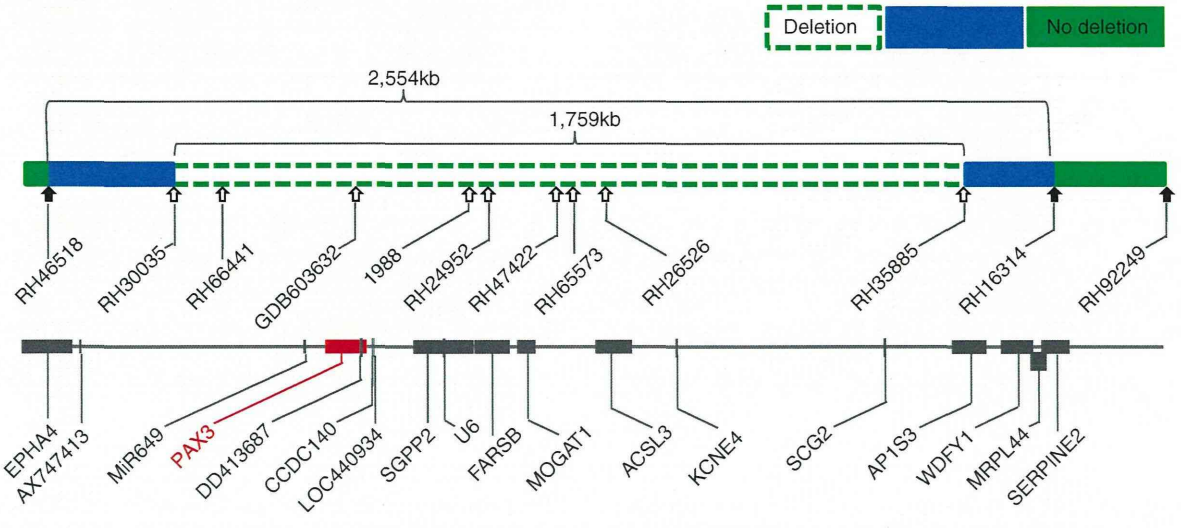

Figure 6. Genetic map showing the estimated location of the *PAX3* deletion together with the regions surrounding *PAX3*. Sites examined by quantitative PCR are indicated by arrows. Blank and white arrows indicate that the quantities of DNA at these sites are half or identical to the quantities of DNA at the corresponding sites in the control, respectively. The 5′ and 3′ ends of the deletion are located within the blue regions flanking the white region, designated as 'deletion,' and flanked by the green regions, designated as 'no deletion.' All genes mapped within this region, including *PAX3*, are shown in the lower map.

its location in *PAX3*, and the severity of the WS1 phenotype [19,20]. Similarly, no evidence of such a correlation was found in the data presented in this study.

In the present study, *PAX3* genetic diagnosis contributed to the accurate diagnosis of WS1. Such diagnosis could help provide genetic counseling to patients with isolated or few phenotypic symptoms, those with mild phenotypes or few first-degree relatives, or those who have yet to develop any symptoms. In addition, analysis of the predicted 3D structure of PAX3 facilitated the verification of pathogenicity of a missense mutation, and MLPA analysis increased the sensitivity of genetic diagnosis of WS1.

Acknowledgments

We thank the families that participated in this study. This study was supported by a Grant-in-Aid for Clinical Research from the National Hospital Organization, and by a Health and Labour Sciences Research Grants for Research on Rare and Intractable Diseases from the Ministry of Health, Labour and Welfare of Japan.

Declaration of interest: The authors report no conflicts of interest. The authors alone are responsible for the content and writing of the paper.

References

[1] Read AP, Newton VE. Waardenburg syndrome. J Med Genet 1997;34:656–65.

[2] Farrer LA, Grundfast KM, Amos J, Arnos KS, Asher JH Jr, Beighton P, et al. Waardenburg syndrome (WS) type I is caused by defects at multiple loci, one of which is near ALPP on chromosome 2: first report of the WS consortium. Am J Hum Genet 1992;50:902–13.

[3] Liu XZ, Newton VE, Read AP. Waardenburg syndrome type II: phenotypic findings and diagnostic criteria. Am J Med Genet 1995;55:95–100.

[4] Pardono E, van Bever Y, van den Ende J, Havrenne PC, Iughetti P, Maestrelli SR, et al. Waardenburg syndrome: clinical differentiation between types I and II. Am J Med Genet A 2003;117A:223–35.

[5] Pingault V, Ente D, Dastot-Le Moal F, Goossens M, Marlin S, Bondurand N. Review and update of mutations causing Waardenburg syndrome. Hum Mutat 2010;31: 391–406.

[6] Milunsky JM, Maher TA, Ito M, Milunsky A. The value of MLPA in Waardenburg syndrome. Genet Test 2007;11:179–82.

[7] Ishikiriyama S, Tonoki H, Shibuya Y, Chin S, Harada N, Abe K, et al. Waardenburg syndrome type I in a child with de novo inversion (2)(q35q37.3). Am J Med Genet 1989;33: 505–7.

[8] Soejima H, Fujimoto M, Tsukamoto K, Matsumoto N, Yoshiura KI, Fukushima Y, et al. Three novel PAX3 mutations observed in patients with Waardenburg syndrome type 1. Hum Mutat 1997;9:177–80.

[9] Kashima T, Akiyama H, Kishi S. Asymmetric severity of diabetic retinopathy in Waardenburg syndrome. Clin Ophthalmol 2011;5:1717–20.

[10] Kiefer F, Arnold K, Kunzli M, Bordoli L, Schwede T. The SWISS-MODEL Repository and associated resources. Nucleic Acids Res 2009;37:D387–92.

[11] Xu W, Rould MA, Jun S, Desplan C, Pabo CO. Crystal structure of a paired domain-DNA complex at 2. 5 A resolution reveals structural basis for Pax developmental mutations. Cell 1995;80:639–50.

[12] Pettersen EF, Goddard TD, Huang CC, Couch GS, Greenblatt DM, Meng EC, et al. UCSF Chimera – a visualization system for exploratory research and analysis. J Comput Chem 2004;25:1605–12.

[13] Chalepakis G, Goulding M, Read A, Strachan T, Gruss P. Molecular basis of splotch and Waardenburg Pax-3-mutations. Proc Natl Acad Sci USA 1994;91:3685–9.

[14] Corry GN, Underhill DA. Pax3 target gene recognition occurs through distinct modes that are differentially affected by disease-associated mutations. Pigment Cell Res 2005;18: 427–38.

[15] Fortin AS, Underhill DA, Gros P. Reciprocal effect of Waardenburg syndrome mutations on DNA binding by the Pax-3 paired domain and homeodomain. Hum Mol Genet 1997;6:1781–90.

[16] Baldwin CT, Lipsky NR, Hoth CF, Cohen T, Mamuya W, Milunsky A. Mutations in PAX3 associated with Waardenburg syndrome type I. Hum Mutat 1994;3:205–11.

[17] Tassabehji M, Newton VE, Leverton K, Turnbull K, Seemanova E, Kunze J, et al. PAX3 gene structure and mutations: close analogies between Waardenburg syndrome and the Splotch mouse. Hum Mol Genet 1994;3: 1069–74.

[18] Wang J, Li S, Xiao X, Wang P, Guo X, Zhang Q. PAX3 mutations and clinical characteristics in Chinese patients with Waardenburg syndrome type 1. Mol Vis 2010;16:1146–53.

[19] Baldwin CT, Hoth CF, Macina RA, Milunsky A. Mutations in PAX3 that cause Waardenburg syndrome type I: ten new mutations and review of the literature. Am J Med Genet 1995;58:115–22.

[20] Tassabehji M, Newton VE, Liu XZ, Brady A, Donnai D, Krajewska-Walasek M, et al. The mutational spectrum in Waardenburg syndrome. Hum Mol Genet 1995;4: 2131–7.

Biochemical and Biophysical Research Communications 432 (2013) 475–479

Contents lists available at SciVerse ScienceDirect

Biochemical and Biophysical Research Communications

journal homepage: www.elsevier.com/locate/ybbrc

Moderate hearing loss associated with a novel KCNQ4 non-truncating mutation located near the N-terminus of the pore helix

Takahisa Watabe [a], Tatsuo Matsunaga [b,*], Kazunori Namba [b], Hideki Mutai [b], Yasuhiro Inoue [a], Kaoru Ogawa [a]

[a] Department of Otolaryngology, Head and Neck Surgery, Keio University, School of Medicine, 35 Shinanomachi, Shinjuku, Tokyo 160-8582, Japan
[b] The Laboratory of Auditory Disorders, National Institute of Sensory Organs, National Tokyo Medical Center, 2-5-1 Higashigaoka, Meguro, Tokyo 152-8902, Japan

ARTICLE INFO

Article history:
Received 28 January 2013
Available online 9 February 2013

Keywords:
KCNQ4
Nonsyndromic hearing loss
Dominant negative effect
Haploinsufficiency
Molecular modeling

ABSTRACT

Genetic mutation is one of the causative factors for idiopathic progressive hearing loss. A patient with late-onset, moderate, and high-frequency hearing loss was found to have a novel, heterozygous *KCNQ4* mutation, c.806_808delCCT, which led to a p.Ser260del located between S5 and the pore helix (PH). Molecular modeling analysis suggested that the p.Ser269del mutation could cause structural distortion and change in the electrostatic surface potential of the *KCNQ4* channel protein, which may impede K+ transport. The present study supports the idea that a non-truncating mutation around the N-terminus of PH may be related to moderate hearing loss.

1. Introduction

Currently, 50 loci and 27 responsible genes for autosomal dominant non-syndromic hearing loss (DFNA) have been identified [1]. *KCNQ4* is one gene that can cause DFNA, type 2 (DFNA2, OMIM: 600101) [2,3]. Patients with mutations in this gene present progressive sensorineural hearing loss starting in the high frequency range. *KCNQ4* (OMIM: 603537) is a voltage-gated KQT-like potassium channel. It modulates the resting membrane potential of the outer hair cells, a type of auditory sensory cell. A functional *KCNQ4* channel consists of four subunits. Each subunit contains six putative domains that span the cellular membrane (S1–S6), a K+-selective pore region consisting of S5, S6, a pore helix (PH), and a pore-loop (P-loop) domain, and N- and C-terminal regions [3].

So far, 11 missense mutations, one nonsense mutation, and three small deletion mutations in *KCNQ4* have been reported to be associated with hearing loss. Understanding the molecular pathology resulting from each *KCNQ4* mutation would be beneficial in predicting the clinical course of KCNQ-related hearing loss. *KCNQ4* mutations can be divided into non-truncating and truncating mutations (Table 1). Most of the *KCNQ4* non-truncating mutations in the pore region are associated with severe hearing loss, except for a non-truncating mutation at the N-terminus of PH, p.Tyr270His, which has been associated with moderate hearing loss [13]. In an electrophysiological study, co-expression of wild-type *KCNQ4* with each non-truncating mutation associated with severe hearing loss, including p.Leu274His, p.Trp276Ser, p.Leu281-Ser, p.Gly285Cys, p.Gly285Ser, p.Gly296Ser, p.Gly321Ser, and p.Gly322_Leu327del, has been shown to result in significantly reduced or non-detectable current [14]. These results indicate that the severe hearing loss in patients carrying these heterozygous mutations is due to a dominant negative effect. On the other hand, the protein products of two *KCNQ4*-truncating mutations, p.Gln71SerfsX138 and p.Gln71fs, lack structural motifs, such as transmembrane domains, and are probably not synthesized from these alleles. Moderate hearing loss in patients carrying these mutations in the heterozygous allele has been considered to be due to haploinsufficiency [3,11].

We identified a novel heterozygous *KCNQ4* non-truncating mutation, c.806_808delCCT, that leads to deletion of a serine residue at position 269 (p.Ser269del), located in the region between S5 and the PH of the protein. Unlike other patients with *KCNQ4* non-truncating mutations, the patient who carried this mutation presented moderate hearing loss. Previously, we reported that a patient having *KCNQ4* with p.Try270His, which is located next to Ser269, showed moderate hearing loss [13], raising the possibility that mutation at or proximal to the N-terminus of PH is associated

Abbreviations: DFNA2, nonsyndromic autosomal dominant sensorineural deafness type 2; *KCNQ4*, potassium voltage-gated channel; KQT-like subfamily, member 4; ABR, auditory brainstem response.

* Corresponding author. Fax: +81 3 3412 9811.
E-mail address: matsunagatatsuo@kankakuki.go.jp (T. Matsunaga).

0006-291X/$ - see front matter © 2013 Elsevier Inc. All rights reserved.
http://dx.doi.org/10.1016/j.bbrc.2013.01.118

Table 1
KCNQ4 mutations affecting the pore region of the channel protein in DFNA2 families.

	Exon		Nucleotide	Amino acid	Protein domain	Onset (y)	Progression	Severity	Mechanism	Refs.
Non-truncating mutation	5	Missense	c.778G>A	p.Glu260Lys	S5	1–20	Yes	SV	Unknown	[9]
	5		c.785A>T	p.Asp262Val	S5-PH	1–20	Yes	SV	Unknown	[9]
	5		c.808T>C	p.Tyr270His	N-terminus of PH	0	Yes	MD	Unknown	[13]
	5		c.821T>A	p.Leu274His	PH	1–20	Yes	SV	D.N.E.	[12]
	5		c.827G>C	p.Trp276Ser	PH	1–20	Yes	SV	D.N.E.	[3–5]
	6		c.842T>C	p.Leu281Ser	PH	1–20	Yes	SV	D.N.E.	[6]
	6		c.853G>T	p.Gly285Cys	P-loop	1–20	Yes	SV	D.N.E.	[3]
	6		c.853G>A	p.Gly285Ser	P-loop	1–20	Yes	SV	D.N.E.	[2]
	6		c.859G>C	p.Gly287Arg	P-loop	1–20	Yes	SV	D.N.E.	[7]
	6		c.886G>A	p.Gly296Ser	S6	1–20	Yes	SV	D.N.E.	[8]
	7		c.961G>A	p.Gly321Ser	S6	1–20	Yes	SV	D.N.E.	[3]
	4	Deletion	c.664_681del18	p.Gly322_Leu327del	S5	1–20	Yes	SV	D.N.E.	[10]
	5		c.806_808del3	p.Ser269del	S5-PH	1–20	Yes	MD	See discussion	This study
Truncating mutation	1	Deletion	c.211del1	p.Gln71SerfsX138	N-terminal cytoplasmic	Unknown	Yes	MD	H.I.?	[11]
	1		c.212_224del13	p.Gln71fs	N-terminal cytoplasmic	1–20	Yes	MD	H.I.?	[3]
	5	Nonsense	c.725G>A	p.Trp242X	S5	1–20	Unknown	SV	Unknown	[9]

SV: severe, MD: moderate D.N.E.: dominant negative effect, H.I.: haploinsufficiency, PH: pore helix.

with moderate hearing loss. In this study, we used molecular modeling to elucidate the molecular mechanism underlying moderate hearing loss associated with *KCNQ4* harboring the p.Ser269del mutation.

2. Materials and methods

2.1. Subjects

All procedures were approved by the Ethics Review Committee of National Mie Hospital and National Tokyo Medical Center, and were conducted after written informed consent had been obtained from each individual.

2.2. Clinical analysis

Hearing level was measured by pure tone audiometry and evaluated by averaging four frequencies, 500, 1000, 2000, and 4000 Hz in the better hearing ear and was classified according to the criteria of GENDEAF (moderate, 41–70 dB; severe, 71–95 dB) [1]. Clinical information, such as age of onset and presence of progression, was gathered from the medical records. Computed tomography (CT) and magnetic resonance imaging (MRI) were done to check whether the patient had an inner ear anomaly and/or retrocochlear disease. Auditory brainstem response (ABR) and distortion product otoacoustic emission (DPOAE) were also examined to evaluate inner ear function.

2.3. Genetic analysis

KCNQ4 was selected as the candidate gene on the basis of clinical features, including onset of hearing loss, audiogram patterns, imaging studies, and hereditary pattern [15]. Prior to this study, the patient was confirmed to have neither GJB2 mutations, the most common causative gene of hereditary hearing loss, nor mitochondrial m.1555A>G and m.3243A>G mutations. Genomic DNA was extracted from blood samples using the Gentra Puregene Blood kit (QIAGEN, Hamburg, Germany). PCR primers specific for *KCNQ4* (GenBank NG_008139, NCBI Build37.1) were selected from the resequencing amplicon probe sets (NCBI). All of the exons, together with the flanking intronic regions, of *KCNQ4* were analyzed by bidirectional sequencing using an ABI 3730 Genetic Analyzer (Applied Biosystems, CA, USA) and the ABI Prism Big Dye Terminator Cycle Sequencing kit (Applied Biosystems). The sequences were characterized using SeqScape software v.2.6 (Applied Biosystems) and DNASIS Pro (Hitachisoft, Tokyo, Japan). Control DNA was obtained from 96 Japanese subjects with normal hearing.

2.4. Molecular model analysis

To predict the effects of the mutation on the KCNQ4 channel, molecular modeling of KCNQ4 was performed as previously described [13]. The crystal structure of Kv1.2 (PDB ID: 3LUT, chain B) [16] was used as the structural template for modeling of the *KCNQ4* sequence based on sequence homology as determined through Gapped BLAST [17] and PDBsum [18]. The pore regions of wild-type KCNQ4 and the p.Ser269del mutation were modeled using SWISS-MODEL Workspace [19] and validated using the Verify 3D Structure Evaluation server [20,21]. The models were each superimposed onto Kv1.2 using Chimera [22] to visualize ribbon models with electrostatic surface potentials and the hydrogen bonds of either wild-type KCNQ4 or KCNQ4 with the p.Ser269del mutation.

3. Results

3.1. Clinical features

The proband was a 25-years-old female in a pedigree of autosomal dominant progressive hearing loss (Fig. 1A). She has become conscious of progressive bilateral hearing loss, since she has become 20 years-old. At 24 years-old, severe mixed hearing loss with high frequency dominance was found in the right ear by pure tone audiometry. An air-bone gap was considered to have resulted from an operation for a right cholesteatoma at 8 years of age. Moderate sensorineural hearing loss with high frequency dominance was found in the left ear (Fig. 1B). No other symptoms accompanying the hearing loss were identified. ABR showed a threshold of 90 dB in the left ear, and no response at 90 dB in the right ear. DPOAE showed a response only at 1000 Hz in the left ear and no response in the right ear. CT and MRI failed to reveal deformity of the inner ear or structural abnormality in the central auditory pathway.

3.2. Novel mutation of KCNQ4

Sequencing analysis of *KCNQ4* from the patient identified a heterozygous deletion of three nucleotides, CCT, at position 806–808 (c.806_808delCCT). The deletion mutation causes a change of amino acid residues from Ser268-Ser269-Tyr270 to Ser268-Tyr269 (p.Ser269del) without a frameshift (Fig. 2A). Ser269 was located

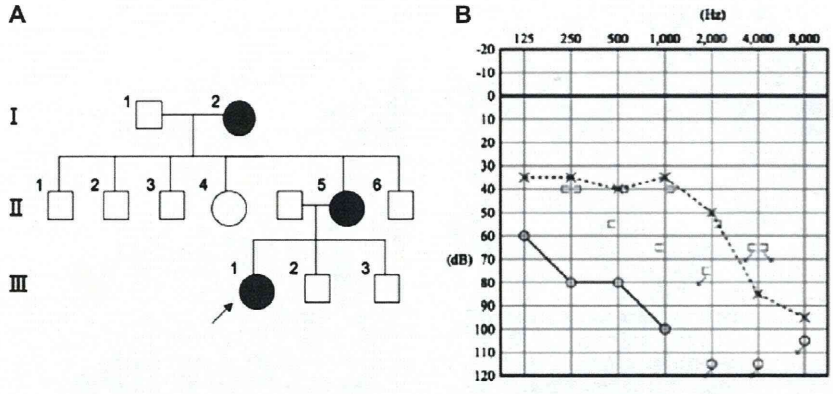

Fig. 1. Clinical information. (A) Pedigree of a family carrying heterozygous *KCNQ4* with the c.806_808delCCT (p.Ser269del) mutation. Individuals with hearing loss are indicated by filled symbols. The arrow indicates the proband. (B) Pure tone audiogram from the proband at 25 years old. Open circles with line: air conduction thresholds of the right ear; x with dotted line: air conduction thresholds of the left ear; left bracket: bone conduction thresholds of the right ear; right bracket: bone conduction thresholds of the left ear. Arrows indicate the non-detectable hearing level by profound hearing loss.

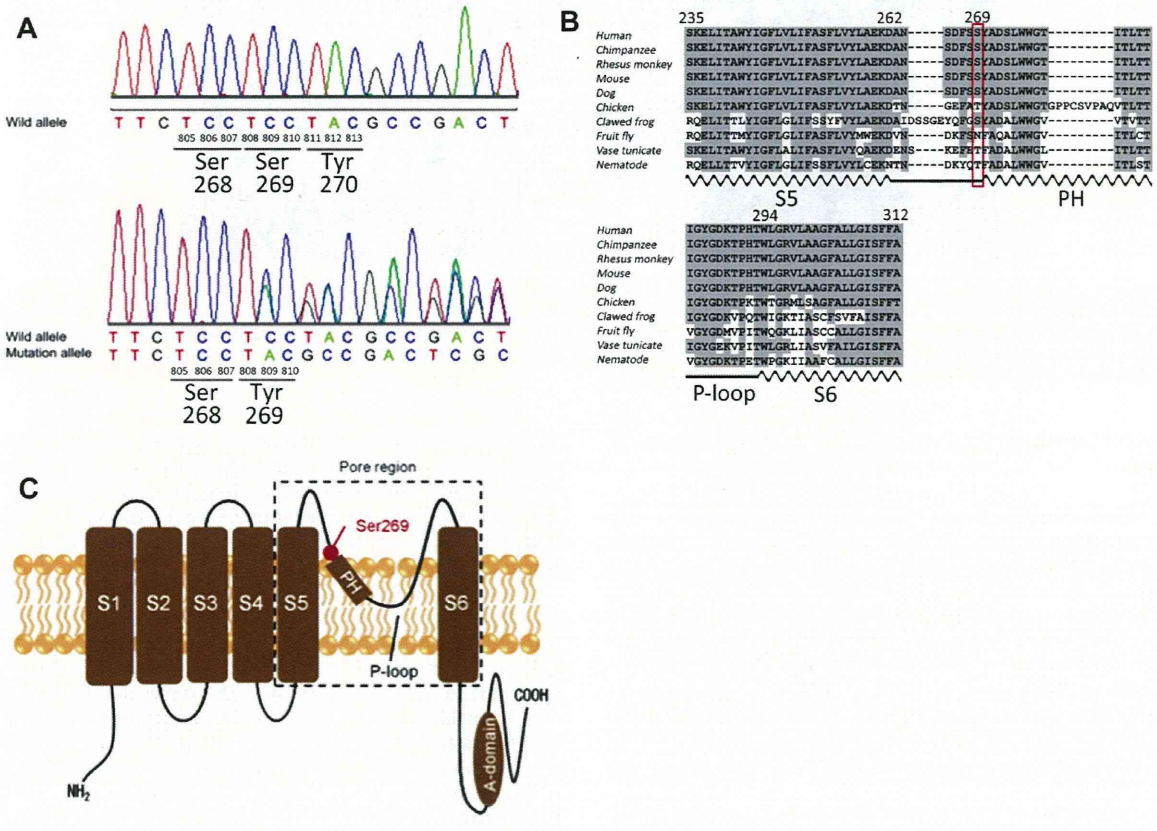

Fig. 2. Partial electrophoretogram of exon 5 of *KCNQ4* with the partial protein sequence for *KCNQ4*. (A) A partial electrophoretogram of exon 5 of *KCNQ4* from an individual with normal hearing (above) and the proband with the heterozygous c.806–808delCCT mutation (below). The positions of the heterozygotic deletion of CCT at 806–808 and the resulting amino acid deletion (p.Ser269del) are indicated. (B) Sequences of the orthologous *KCNQ4* pore region are aligned. Positions highlighted in gray indicate the residues identical to human *KCNQ4*. The position of Ser269 is enclosed by a red square. The positions of S5, pore helix (PH), S6 (wavy lines) and the P-loop (straight line) are shown below the sequences. (C) Schematic topology of *KCNQ4*. Putative domains, including transmembrane regions (S1-S6), channel pore region, PH, P-loop, and A-domain are indicated. Position of Ser269 is indicated by a red circle. (For interpretation of the references to color in this figure legend, the reader is referred to the web version of this article.)

in the region between the putative S5 and PH, a highly conserved region among animal species (Fig. 2B and C). This mutation was found neither on the Exome Variant Server [23] nor in the control group of 96 unrelated Japanese individuals with normal hearing.

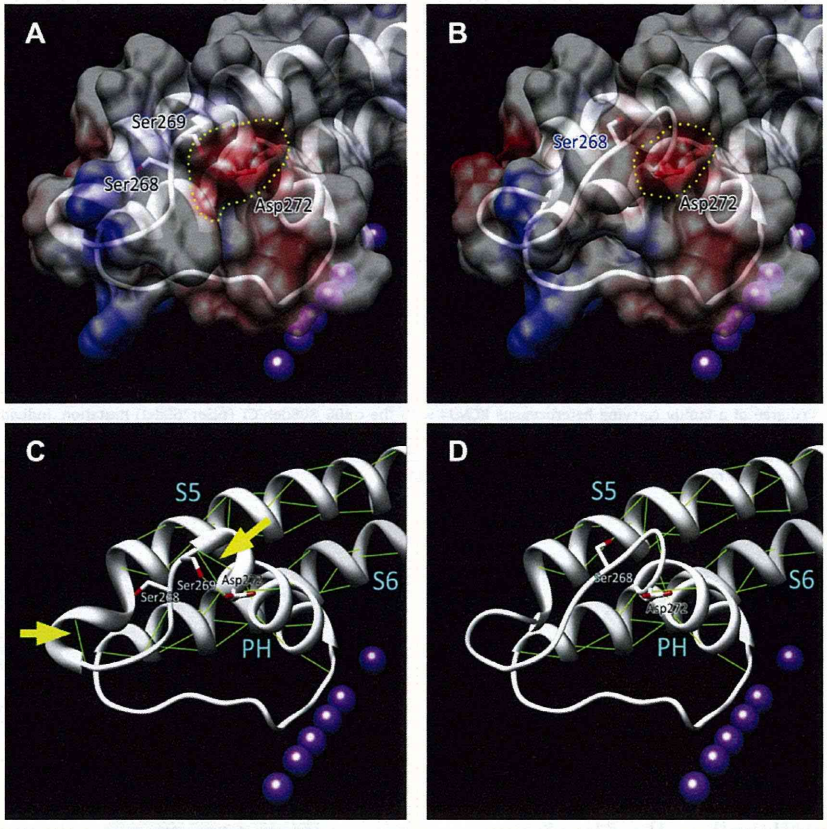

Fig. 3. Partial structural model of KCNQ4 and the p.Ser269del mutation. (A and B) The ribbon models of (A) wild-type KCNQ4 subunit and (B) KCNQ4 subunit with the p.Ser269del mutation overlaid with their corresponding electrostatic surface potential. Red or blue area: negatively or positively charged residues, yellow dot circle: negatively charged surface potential on the N-terminal region of the pore helix (PH). (C and D) Ribbon models of (C) wild-type KCNQ4 and (D) KCNQ4 with the p.Ser269del mutation. Green lines: putative hydrogen bonds; yellow arrows: hydrogen bonds within S5 and PH; purple spheres: potassium ions. (For interpretation of the references to color in this figure legend, the reader is referred to the web version of this article.)

3.3. Predicted structural change in KCNQ4 caused by the p.Ser269del mutation

The ribbon model of the wild-type KCNQ4 subunit overlaid with the corresponding electrostatic surface potential demonstrated that the surface of the N-terminal region of PH is negatively charged because of the negatively charged side chains of Ser269 and Asp272 (Fig. 3A). The model of KCNQ4 with the p.Ser269del mutation demonstrated reduction of the negatively charged surface area in this region (Fig. 3B). Reduction of the electrostatic surface potential in this area has been predicted to impede K+ transport because of the long range electrostatic attractive force between PH and K+ [13]. In addition, hydrogen bonds on the C-terminus of S5 and the N-terminus of PH of wild-type KCNQ4 (Fig. 3C, yellow arrows) were absent in KCNQ4 with the Ser269del mutation (Fig. 3D). Loss of the hydrogen bonds around the N-terminus of PH resulted in shortening of the PH and was attributed to destabilization of α-helix formation [24]. The disrupted helices would affect the structural stability of the pore region and lead to abnormal channel function.

4. Discussion

Most of the *KCNQ4* non-truncating mutations affecting the pore region are associated with severe hearing loss. However, we found that the non-truncating p.Tyr270His [14] and p.Ser269del mutations were associated with moderate hearing loss. *KCNQ4* mutations at or proximal to the N-terminus of PH are suggested to be associated with moderate hearing loss, because this site is predicted to have relatively smaller influence than other pore regions, such as S5, S6, the central region of PH, and the P-loop, on KCNQ4 channel function.

The molecular pathology associated with the p.Ser269del mutation, demonstrated in silico, indicates a reduction in the negatively charged electrostatic surface potential and structural distortion of the pore region by the mutated KCNQ4, which may explain the associated moderate hearing loss. The molecular mechanism in this case is likely to be a mild dominant negative effect resulting from the relatively small influence of *KCNQ4* with the p.Ser269del mutation on the normal channel subunit. However, another possibility is haploinsufficiency resulting from the loss of function of *KCNQ4* with the p.Ser269del mutation. This scenario, which would not affect the functioning of the other channel subunits, cannot be excluded.

5. Conclusion

We found a novel heterozygous *KCNQ4* mutation, c.806_808delCCT (p.Ser269del), in a pedigree with progressive and moderate hearing loss. Molecular modeling analysis of this mutation demonstrated that changes in electrostatic surface potential and structural distortion could be relevant to the pathology underlying

auditory dysfunction. Mutations at or proximal to the N-terminus of the PH of the KCNQ4 channel might cause mild molecular dysfunction and be associated with moderate hearing loss.

Acknowledgment

This study was supported by a Grant-in-Aid for Clinical Research from the National Hospital Organization.

References

[1] <http://hereditaryhearingloss.org/> (accessed September 2012).
[2] C. Kubisch, B.C. Schroeder, T. Friedrich, B. Lütjohann, A. El Amraoui, S. Marlin, C. Petit, T.J. Jentsch, KCNQ4, a novel potassium channel expressed in sensory outer hair cells, is mutated in dominant deafness, Cell 96 (1999) 437–446.
[3] P.J. Coucke, P. Van Hauwe, P.M. Kelley, H. Kunst, I. Schatteman, D. Van Velzen, J. Meyers, R.J. Ensink, M. Verstreken, F. Declau, H. Marres, K. Kastury, S. Bhasin, W.T. McGuirt, R.J. Smith, C.W. Cremers, P. Van de Heyning, P.J. Willems, S.D. Smith, G. Van Camp, Mutations in the KCNQ4 gene are responsible for autosomal dominant deafness in four DFNA2 families, Hum. Mol. Genet. 8 (1999) 1321–1328.
[4] J. Akita, S. Abe, H. Shinkawa, W.J. Kimberling, S. Usami, Clinical and genetic features of nonsyndromic autosomal dominant sensorineural hearing loss: KCNQ4 is a gene responsible in japanese, J. Hum. Genet. 46 (2001) 355–361.
[5] G. Van Camp, P.J. Coucke, J. Akita, E. Fransen, S. Abe, E.M. De Leenheer, P.L. Huygen, C.W. Cremers, S. Usami, A mutational hot spot in the KCNQ4 gene responsible for autosomal dominant hearing impairment, Hum. Mutat. 20 (2002) 15–19.
[6] Z. Talebizadeh, P.M. Kelley, J.W. Askew, K.W. Beisel, S.D. Smith, Novel Mutation in the KCNQ4 Gene in a large kindred with dominant progressive hearing loss, Hum. Mutat. 14 (1999) 493–501.
[7] J. Arnett, S.B. Emery, T.B. Kim, A.K. Boerst, K. Lee, S.M. Leal, M.M. Lesperance, Autosomal dominant progressive sensorineural hearing loss due to a novel mutation in the KCNQ4 gene, Arch. Otolaryngol. Head Neck Surg. 137 (2011) 54–59.
[8] A. Mencía, D. González-Nieto, S. Modamio-Høybjør, A. Etxeberría, G. Aránguez, N. Salvador, I. Del Castillo, A. Villarroel, F. Moreno, L. Barrio, M.A. Moreno-Pelayo, A novel KCNQ4 pore-region mutation (p.G296S) causes deafness by impairing cell-surface channel expression, Hum. Genet. 123 (2008) 41–53.
[9] M.S. Hildebrand, D. Tack, S.J. McMordie, A. DeLuca, I.A. Hur, C. Nishimura, P. Huygen, T.L. Casavant, R.J. Smith, Audioprofile-directed screening identifies novel mutations in KCNQ4 causing hearing loss at the DFNA2 locus, Genet. Med. 10 (2008) 797–804.
[10] J.I. Baek, H.J. Park, K. Park, S.J. Choi, K.Y. Lee, J.H. Yi, T.B. Friedman, D. Drayna, K.S. Shin, U.K. Kim, Pathogenic effects of a novel mutation (c.664_681del) in KCNQ4 channels associated with auditory pathology, Biochim. Biophys. Acta 2011 (1812) 536–543.
[11] F. Kamada, S. Kure, T. Kudo, Y. Suzuki, T. Oshima, A. Ichinohe, K. Kojima, T. Niihori, J. Kanno, Y. Narumi, A. Narisawa, K. Kato, Y. Aoki, K. Ikeda, T. Kobayashi, Y. Matsubara, A novel KCNQ4 one-base deletion in a large pedigree with hearing loss: implication for the genotype-phenotype correlation, J. Hum. Genet. 51 (2006) 455–460.
[12] P. Van Hauwe, P.J. Coucke, R.J. Ensink, P. Huygen, C.W. Cremers, G. Van Camp, Mutations in the KCNQ4 K+ channel gene, responsible for autosomal dominant hearing loss, cluster in the channel pore region, Am. J. Med. Genet. 93 (2000) 184–187.
[13] K. Namba, H. Mutai, H. Kaneko, S. Hashimoto, T. Matsunaga, In silico modeling of the pore region of a KCNQ4 missense mutant from a patient with hearing loss, BMC Res. Notes 5 (2012) 145.
[14] H.J. Kim, P. Lv, C.R. Sihn, E.N. Yamoah, Cellular and molecular mechanisms of autosomal dominant form of progressive hearing loss, DFNA2, J. Biol. Chem. 286 (2011) 1517–1527.
[15] T. Matsunaga, Value of Genetic testing in the ontological approach for sensorineural hearing loss, Keio J. Med. 58 (2009) 216–222.
[16] X. Chen, Q. Wang, F. Ni, J. Ma, Structure of the full-length shaker potassium channel Kv1.2 by normal-mode-based X-ray crystallographic refinement, Proc. Natl. Acad. Sci. USA 107 (2010) 11352–11357.
[17] S.F. Altschul, T.L. Madden, A.A. Schäffer, J. Zhang, Z. Zhang, W. Miller, D.J. Lipman, Gapped BLAST and PSI-BLAST: a new generation of protein database search programs, Nucleic Acids Res. 25 (1997) 3389–3402.
[18] R.A. Laskowski, Enhancing the functional annotation of PDB structures in PDBsum using key figures extracted from the literature, Bioinformatics 23 (2007) 1824–1827.
[19] <http://swissmodel.expasy.org/> (accessed November 2012).
[20] <http://nihserver.mbi.ucla.edu/Verify_3D> (accessed November 2012).
[21] K. Arnold, L. Bordoli, J. Kopp, T. Schwede, The SWISS-MODEL workspace: a web-based environment for protein structure homology modeling, Bioinformatics 22 (2006) 195–201.
[22] E.F. Pettersen, T.D. Goddard, C.C. Huang, G.S. Couch, D.M. Greenblatt, E.C. Meng, T.E. Ferrin, UCSF Chimera – a visualization system for exploratory research and analysis, J. Comput. Chem. 25 (2004) 1605–1612.
[23] <http://evs.gs.washington.edu/EVS/> (accessed August 2012).
[24] W.G. Hol, Effects of the alpha-helix dipole upon the functioning and structure of proteins and peptides, Adv. Biophys. 19 (1985) 133–165.

Pendred症候群研究の現況と展望

Current status and perspectives of the research in Pendred syndrome

松永達雄[1]　藤岡正人[2,3]　細谷　誠[3]

Abstract

Pendred syndrome is an autosomal recessive disorder characterized by sensorineural hearing loss, goiter, and a partial defect in iodide organification, and is the most common syndromic hearing loss. Hearing loss is congenital in most cases and is accompanied by an enlarged vestibular aqueduct and a Mondini cochlea. Pendred syndrome and autosomal recessive deafness-4(DFNB4) with enlarged vestibular aqueduct comprise a phenotypic spectrum caused by mutations in *SLC26A4*. Recently, mutations in *FOXI1* and *KCNJ10* have also been identified in DFNB4. Molecular mechanism of hearing loss and goiter remains to be elucidated, and therapies which can reverse or prevent the progression of the symptoms are not available. Here, we describe advances in the basic, clinical, and translational studies on Pendred syndrome.

Key words: Pendred syndrome, *SLC26A4*, DFNB4, hereditary hearing loss, enlarged vestibular aqueduct

はじめに

Pendred症候群(OMIM: 274600)は感音難聴，甲状腺腫，ヨード有機化障害を特徴とする常染色体劣性遺伝の疾患である．本症候群は最も頻度の高い症候群性難聴であり，遺伝性難聴全体の5-10％と考えられている[1]．難聴は生下時より高度の場合や，軽度あるいは中等度難聴から進行する場合など様々であり，頭部への衝撃などによって難聴の急性増悪が生じることも多い．先天性あるいは小児期からの難聴は言語発達，教育，社会参加に重大な影響を与えるため，早期発見とそれに続く言語聴覚リハビリテーションの実施が極めて重要である．しかし，本症候群の患者は検査やリハビリテーションへの協力が十分できない乳幼児である場合が多く，更に難聴の変動，進行も多いことから，医学的対応が困難な場合が多い．甲状腺腫は思春期前後から成人後早期に発症するが，大多数は甲状腺機能低下症を伴わない．前庭機能低下も認められ，一部の患者ではめまい発作を反復する．本症候群の患者では，CTやMRIの画像検査で内耳に前庭水管拡大とMondini奇形(蝸牛低形成)が認められることが大きな特徴である．

Pendred症候群の主要な原因は*SLC26A4*遺伝子変異である[2]．一方で*SLC26A4*遺伝子変異は，感音難聴のみを発症して甲状腺腫を伴わない非症候群性難聴DFNB4(OMIM: 600791)の

[1]Tatsuo Matsunaga, [2,3]Masato Fujioka, [3]Makoto Hosoya: [1]Department of Otolaryngology/Laboratory of Auditory Disorders, National Institute of Sensory Organs, National Tokyo Medical Center　独立行政法人国立病院機構東京医療センター　耳鼻咽喉科/感覚器センター　聴覚障害研究室　[2]Department of Otorhinolarygology, Keiyu Hospital　財団法人神奈川警友会けいゆう病院　耳鼻咽喉科　[3]Department of Otorhinolaryngology, Head and Neck Surgery, School of Medicine, Keio University　慶應義塾大学医学部　耳鼻咽喉科・頭頸部外科

0047-1852/13/¥60/頁/JCOPY

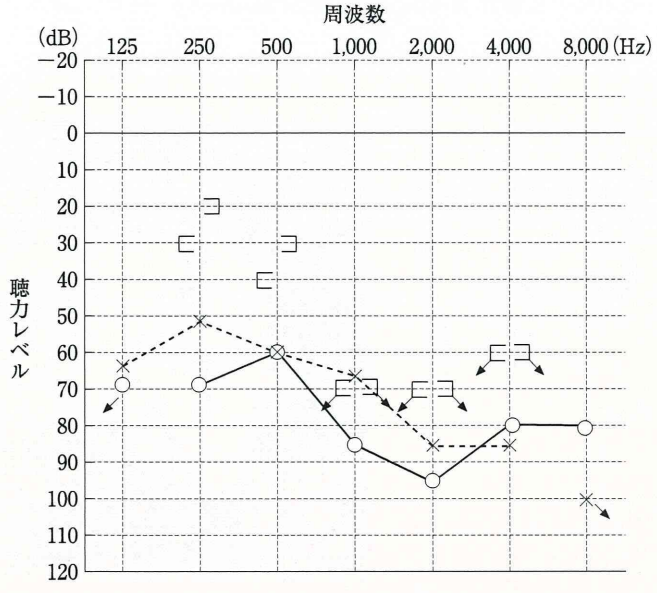

図1　Pendred症候群患者の代表的な純音聴力検査の結果(オージオグラム)
横軸が検査音の周波数，縦軸が各周波数の検査音を聴取できる閾値(聴力レベル)を示す．本症候群の患者では，高音域(高い周波数)の聴力レベルが低い．低音域(低い周波数)の気導聴力閾値と骨導聴力閾値に差がある(気骨導差)．○：右耳の気導聴力閾値，×：左耳の気導聴力閾値，⊏：右耳の骨導聴力閾値，⊐：左耳の骨導聴力閾値．

原因でもある[3]．DFNB4も劣性遺伝であり，画像検査では前庭水管拡大を認め，Mondini奇形を伴う場合も多い．現在，Pendred症候群とDFNB4は同一疾患の表現型の違いとして考えられている[4]．

1. Pendred症候群の診療

Pendred症候群の臨床診断は，①感音難聴，②両側性前庭水管拡大，③パークロレート放出試験の異常または甲状腺腫をもって確定診断とする[5]．一方，DFNB4の臨床診断では①感音難聴，②前庭水管拡大，③甲状腺機能正常により確定する．

感音難聴は年齢に応じた聴力検査で判定される．本症候群の難聴の特徴として，高い音に対する反応の顕著な低下が認められる(**図1**)．急性増悪や回復を繰り返す場合も多く，徐々に進行して低い音から高い音までの全音域で反応が失われることもある．低音域に通常は伝音難聴(中耳や外耳の問題による難聴)でしか認められない骨導閾値と気導閾値の差がみられるため，診断に苦慮する場合がある．前庭水管拡大は側頭骨CTあるいは内耳MRIで，前庭水管の中間径が1.5 mm以上あるいは中頭蓋窩開口部径が2 mm以上あると拡大と判定される(**図2-a**，**b**)．最近，著者らはPendred症候群の患者において前庭水管拡大の形態的特徴と*SLC26A4*遺伝子変異の種類および難聴の特徴が関連していないことを報告した[6]．

パークロレート放出試験では甲状腺におけるヨード有機化障害を判定する．Pendred症候群ではヨード有機化障害を認め陽性となる．パークロレート放出試験は放射性物質を用いる検査であるため，現在は実施している施設が極めて少ない．また，特異性と感度に問題が生じる場合が比較的多く，判定基準も統一されていないことなどからも，実施されない患者が多い．これに代わって近年は，Pendred症候群の主要な原因である*SLC26A4*遺伝子の検査で遺伝子診断される患者が増加している．